Journal of Solid State Chemistry 182 (2009) 778–789

Contents lists available at ScienceDirect

Journal of Solid State Chemistry

journal homepage: www.elsevier.com/locate/jssc

Networks of icosahedra in the sodium–zinc–stannides $Na_{16}Zn_{13.54}Sn_{13.46(5)}$, $Na_{22}Zn_{20}Sn_{19(1)}$, and $Na_{34}Zn_{66}Sn_{38(1)}$

Sung-Jin Kim, Thomas F. Fässler *

Department of Chemistry, Technische Universität München, Lichtenbergstr. 4, D-85747 Garching, Germany

ARTICLE INFO

Article history:
Received 16 September 2008
Received in revised form
15 December 2008
Accepted 28 December 2008
Available online 6 January 2009

Keywords:
Tin
Zinc
Intermetallics
Crystal chemistry
Cluster

ABSTRACT

The three new ternary phases $Na_{16}Zn_{13.54}Sn_{13.46(5)}$ (**I**), $Na_{22}Zn_{20}Sn_{19(1)}$ (**II**), and $Na_{34}Zn_{66}Sn_{38(1)}$ (**III**) were obtained by direct fusion of the pure elements and characterized by single crystal X-ray diffraction experiments: **I**, *Ibam*, $Z=8$, $a=27.401(1)$, $b=16.100(1)$, $c=18.431(1)$ Å, R_1/wR_2 (all data) = 0.051/0.088; **II**, *Pnma*, $Z=4$, $a=16.403(1)$, $b=15.598(1)$, $c=22.655(6)$ Å, R_1/wR_2 (all data) = 0.038/0.071; **III**, $R\bar{3}m$, $Z=3$, $a=16.956(1)$, $c=36.861(1)$ Å, R_1/wR_2 (all data) = 0.045/0.092. The structures consist of complex 3D cluster networks made of Zn and Sn atoms with the common motif of Kagomé nets of icosahedra. Additionally to the new heteroatomic $\{Zn_{12-x}Sn_x\}$ icosahedra that are omnipresent, triangular units, cages, and pairs of triply fused icosahedra fill the cavities of the Kagomé nets in compounds **I**, **II**, and **III**, respectively. Whereas **I** crystallizes in a new structure type, **II** and **III** have structural analogs in trielide chemistry. All three compounds closely approach the electron numbers expected for valence compounds according to the extended 8-N rule. The concept of achieving an isovalent situation to triel elements by combination of electron poorer and richer elements and the readily mixing of Zn and Sn allow the formation of icosahedral and triangular clusters without the participation of a group 13 element.

1. Introduction

Much attention has been centered on semimetal clustering in intermetallic phases [1], in which clusters are mostly fused together due to lack of electrons. The structures can be assembled in one-, two-, or three-dimensions by vertex-linkage, or edge-, vertex-, or face-sharing polyhedra and often the cluster arrangements follow basic principles in analogy to closest atom packing or high coordination numbers as described by Laves [2]. Altogether this results in an enormous variety and diversity of structures which can be of remarkable complexity. The majority of the known examples contains frameworks of triel atoms and clusters and has been extensively studied in the past [3].

In addition to the structural complexity, the problem of the assignment of electrons to the individual building blocks is an interesting issue. Classical valence rules and the rules first described for bonding in borane clusters [4] often can only be applied in more simple cases. With the discovery of new clusters, cages, and aggregates of clusters these rules were extended and have been the subject of intensive computational studies [5]. Those theoretical investigations showed that such phases often exhibit, or closely approach, closed shell electronic configuration as it is usually observed for Zintl phases. Such an electronic situation is attained by fractional occupation or vacancies at specific cluster sites [6]. For example, in $Mg_{35}Cu_{24}Ga_{53}$ [7], $Li_3Na_5Ga_{19.6}$, or $Rb_{0.6}Na_{6.25}Ga_{20.02}$ [8] not all vertices of the polyhedra are fully occupied with Ga atoms, which means that clusters statistically have defects and are of *nido*-, *arachno*-, or even *hypho*-type with respect to the polyhedral skeletal electron pair theory [9]. Besides defect formation the accommodation of the electron demand can also be achieved by partial atom-by-atom substitution with atoms of another group or mimicking a triel element by entirely mixing of group-12 and group-14 elements [10,11].

The most common polyhedron found in trielide structure chemistry is the icosahedron, which can exist as vertex, edge, or face sharing units. Triply fused icosahedra occur as building units in β-boron and also as $\{(Ga/M)_{28}\}$ in $Na_{102}(MGa)_{315}$ (M = Cu, Zn) [12], as $\{(In/T)_{28}\}$ (T = Mg, Zn, Au) in $K_{34}(In/T)_{105}$ [13], and as $\{(In/Li)_{28}\}$ in $K_{34}In_{92.30}Li_{12.70}$ [14]. Clusters or cages without specific symmetry are the electron precise $\{M_{15}\}$ or $\{M_{16}\}$ spacers which are present in moderately reduced phases, such as in $Na_{22}Ga_{39}$ [15], Na_7Ga_{13} [16], and $K_{21.33}In_{39.67}$ [17].

Whereas gallides tend to adjust the optimal electron count by vacancy formation, mixing of group-12 and group-14 elements on the crystallographic gallium position introduces a further degree of freedom (pseudo-atom approach). Changing the statistical ratio of the two atom kinds allows electron count adjustment without

* Corresponding author. Fax: +49 89 289 13186.
E-mail address: thomas.faessler@lrz.tum.de (T.F. Fässler).

0022-4596/$ - see front matter © 2009 Elsevier Inc. All rights reserved.
doi:10.1016/j.jssc.2008.12.023

vacancy formation. In our investigations we concentrate on the *hitherto* scarcely investigated ternary system Na/Zn/Sn. We found a surprisingly rich structural chemistry with structures that are readily tunable by the amount of valence electrons [10,18]. Herein we report about the structures and bonding of the three new intermetallic stannides $Na_{16}Zn_{13.54}Sn_{13.46(5)}$ (**I**), $Na_{22}Zn_{20}Sn_{19(1)}$ (**II**), and $Na_{34}Zn_{66}Sn_{38(1)}$ (**III**).

2. Experimental section

2.1. Syntheses

The compounds were obtained by direct fusion of the commercially obtained elements (Na chunks, Zn rods, Sn drops, all from Merck), which were stored and handled in an Ar-filled glovebox (H_2O and O_2 levels < 0.1 ppm). The chemicals were loaded and enclosed into tantalum ampoules, which afterwards were placed into a silica Schlenk tube. After evacuation the container was exposed to a temperature program. Compound **I** was first obtained from a reaction of the elements at 500 °C with a loading ratio Na:Zn:Sn = 1.00:0.47:0.80. However, in this mixture **I** was only found as a byproduct, besides the main phase $Na_{29}Zn_{24}Sn_{32}$ [10]. According to powder X-ray diffraction data (measured in Debye–Scherrer mode on a Stoe Stadi P) an almost pure phase of the compound, was synthesized by the reaction of stoichiometric amounts (1.00:0.85:0.85) at 500 °C for 6 h, followed by quenching to room temperature, and annealing at 420 °C for 30 days. Single crystals of **II** and **III** were found as byproducts when reacting elemental Na:Zn:Sn in the ratio of 1.00:0.83:1.10 at 500 °C and annealing at 300 °C for four weeks. Powder X-ray measurement and thermal analysis of that mixture indicated the presence of at least two additional phases next to the main phase $Na_{29}Zn_{24}Sn_{32}$. Accommodating reaction loadings to the crystallographically refined compositions of **II** and **III** did not result in higher yields. In powdered samples reflections of **II** and **III** were detected with weak intensities. Up to now these two phases could only be obtained as minor crystalline components and both exhibit block-shaped crystal with metallic luster. All compounds **I**–**III** are air and moisture sensitive.

2.2. X-ray studies and structure refinements

Relevant crystallographic data for compounds **I**, **II**, and **III** are comprised in Table 1. The atomic coordinates and interatomic distance ranges for different atom types are listed in Tables 2 and 3, respectively. A table with selected interatomic distances (Table S2) is included as supplementary data. In the glovebox a silvery block shaped single crystal of each phase was fixed on a glass fiber, sealed into a glass capillary (0.3 mm, Hilgenberg), and measured on an Oxford Xcalibur3 diffractometer (Mo-$K\alpha$ radiation, $\lambda = 0.71073$ Å, graphite monochromator, CCD detector) at room temperature. After applying an empirical absorption correction [19] the structures were solved and refined with SHELX-97 [20]. The data collections for **I** included 416 frames from four ω scans with 1°/frame scan width, detector distance 50 mm and 10 s exposure time. The indexing routine and the systematic absence conditions indicated a body-centered orthorhombic unit cell in the possible space groups *Iba*2 (non-centrosymmetric) and *Ibam* (No. 72). The latter one was chosen due to the best converging model in terms of final residuals, internal *R*-values, and residual electron density. Upon refinement 10 Na, 10 Sn and 7 Zn positions could be assigned. Three sites (M8–M10) showed considerably larger anisotropic displacement parameters (ADPs). Therefore mixed sites with Zn were introduced which led to occupancies for M = Sn/Zn: 0.48/0.52(1) for M8, 0.52/0.48(1) for M9, and 0.49/0.51(1) for M10. This resulted in a significant decrease of final residual electron density. The Sn7 position showed only small amounts of mixing with Zn (98% Sn) and was therefore treated fully as a Sn atom [21].

For **II** and **III** the data collection included 776 frames that were taken in four ω and one φ scan with 30s exposure time and 50 mm detector distance. The space group *Pnma* (No. 62) was assigned based on systematic absence conditions for **II**. From the 18 Sn positions 13 had to be refined considering Sn/Zn mixed occupancies (M1–M13) with Sn occupancies ranging from 14% to 71%. The remaining five Sn (Sn14–Sn18) and five Zn (Zn14–Zn18) did not show significant mixed occupancy. Of the 16 Na atoms only Na16 showed larger ADPs but could not be refined with split positions. Therefore this is ascribed to its poor coordination environment. For **III** the structure could be successfully solved and

Table 1
Single crystal and refinement data for $Na_{16}Zn_{13.54}Sn_{13.46(5)}$ (**I**), $Na_{22}Zn_{20}Sn_{19(1)}$ (**II**), and $Na_{34}Zn_{66}Sn_{38(1)}$ (**III**).

	I	**II**	**III**
fw (g mol^{-1})	2850.72	4057.63	9607.92
Temperature (K)		293(2)	
Diffractometer		Oxford Xcalibur3 (CCD)	
Crystal system	Orthorhombic	Orthorhombic	Trigonal
Space group	*Ibam* (No. 72)	*Pnma* (No. 62)	$R\bar{3}m$ (No. 166)
Unit cell parameters (Å)	$a = 27.401(1)$	$a = 16.403(1)$	
	$b = 16.100(1)$	$b = 15.598(1)$	$a = 16.956(1)$
	$c = 18.431(1)$	$c = 22.655(6)$	$c = 36.861(1)$
Unit cell volume (Å^3); *Z*	8131.2(3); 8	5796.1(1); 4	9177.6(2); 3
ρ_{calc} (g cm^{-3})	4.66	4.65	5.22
μ (mm^{-1}) (Mo $K\alpha$)	16.08	16.27	20.40
Θ range (deg)	2.93–27.81	2.95–27.78	3.55–25.30
Integrated reflections	30990 ($R_\sigma = 0.035$)	83143 ($R_\sigma = 0.019$)	29093 ($R_\sigma = 0.013$)
Independent reflections	4949 ($R_{int} = 0.048$)	7086 ($R_{int} = 0.043$)	2061 ($R_{int} = 0.030$)
Parameters	213	312	139
Goodness of fit on F^2	1.086	1.132	1.310
Observed reflections [$I > 2\sigma(I)$]	3616	5844	1912
R_1/wR_2 [$I > 2\sigma(I)$]	0.033/0.078	0.028/0.065	0.042/0.091
R_1/wR_2 (all data)	0.051/0.088	0.038/0.071	0.045/0.092
Residual map (e$^-$ Å^{-3})	+1.87 [0.80 Å from Zn10]	+2.54 [0.82 Å from Zn10]	+1.59 [1.77 Å from Zn14]
	−2.15 [0.77 Å from Sn7]	−1.80 [0.70 Å from Zn11]	−4.41 [2.63 Å from M5]

Table 2
Atomic coordinates and equivalent isotropic displacement parameters for $Na_{16}Zn_{13.54}Sn_{13.46(5)}$ (**I**), $Na_{22}Zn_{20}Sn_{19(1)}$ (**II**), and $Na_{34}Zn_{66}Sn_{38(1)}$ (**III**).

Atom	Wyck.	Occ.≠1	*x*	*y*	*z*	U_{eq} (Å^2)
I						
Sn1	8*j*		0.1705(1)	0.1600(1)	0	0.013(1)
Sn2	8*j*		0.2561(1)	0.0909(1)	$\frac{1}{2}$	0.013(1)
Sn3	16*k*		0.3300(1)	0.1707(1)	0.0818(1)	0.016(1)
Sn4	8*j*		0.0800(1)	0.0996(1)	$\frac{1}{2}$	0.018(1)
Sn5	16*k*		0.8926(1)	0.3789(1)	0.3436(1)	0.018(1)
Sn6	16*k*		0.1995(1)	0.0953(1)	0.2498(1)	0.016(1)
Sn7	16*k*		0.9870(1)	0.2838(1)	0.3312(1)	0.021(1)
M8 = Sn8/Zn8	16*k*	0.48/0.52(1)	0.0510(1)	0.0017(1)	0.3765(1)	0.016(1)
M9 = Sn9/Zn9	8*f*	0.52/0.48(1)	0.1063(1)	0	$\frac{1}{4}$	0.018(1)
M10 = Sn10/Zn10	16*k*	0.49/0.51(1)	0.9784(1)	0.4280(1)	0.4238(1)	0.027(1)
Zn1	16*k*		0.2294(1)	0.1723(1)	0.1227(1)	0.015(1)
Zn2	8*j*		0.1678(1)	0.1795(1)	$\frac{1}{2}$	0.016(1)
Zn3	8*j*		0.2588(1)	0.0813(1)	0	0.016(1)
Zn4	16*k*		0.1803(1)	0.3077(1)	0.0772(1)	0.017(1)
Zn5	16*k*		0.2263(1)	0.1818(1)	0.3775(1)	0.016(1)
Zn6	16*k*		0.9932(1)	0.1428(1)	0.4244(1)	0.018(1)
Zn7	8*j*		0.0814(1)	0.0823(1)	0	0.016(1)
Na1	8*j*		0.0762(1)	0.2815(3)	0	0.022(1)
Na2	16*k*		0.1695(1)	0.9927(2)	0.9034(2)	0.022(1)
Na3	16*k*		0.1112(1)	0.1729(2)	0.1508(2)	0.022(1)
Na4	16*k*		0.2918(1)	0.0054(2)	0.3467(2)	0.029(1)
Na5	8*g*		0	0.1073(3)	$\frac{1}{4}$	0.028(1)
Na6	16*k*		0.3056(1)	0.1968(2)	0.2538(2)	0.022(1)
Na7	16*k*		0.4222(1)	0.0768(2)	0.1798(2)	0.032(1)
Na8	8*j*		0.0581(2)	0.3041(3)	$\frac{1}{2}$	0.037(1)
Na9	8*j*		0.3726(2)	0.0151(3)	$\frac{1}{2}$	0.035(1)
Na10	16*k*		0.1019(1)	0.1892(2)	0.3418(2)	0.034(1)
II						
M1 = Sn1/Zn1	8*d*	0.49/0.51(1)	0.5997(1)	0.0770(1)	0.4178(1)	0.016(1)
M2 = Sn2/Zn2	8*d*	0.47/0.53(1)	0.3402(1)	0.1607(1)	0.3264(1)	0.015(1)
M3 = Sn3/Zn3	8*d*	0.36/0.64(1)	0.4231(1)	0.0721(1)	0.4094(1)	0.016(1)
M4 = Sn4/Zn4	8*d*	0.43/0.57(1)	0.6426(1)	0.9267(1)	0.4741(1)	0.016(1)
M5 = Sn5/Zn5	8*d*	0.49/0.51(1)	0.2139(1)	0.1488(1)	0.5561(1)	0.019(1)
M6 = Sn6/Zn6	8*d*	0.44/0.56(1)	0.9275(1)	0.0582(1)	0.5609(1)	0.020(1)
M7 = Sn7/Zn7	8*d*	0.14/0.86(1)	0.6390(1)	0.0767(1)	0.5443(1)	0.019(1)
M8 = Sn8/Zn8	8*d*	0.44/0.56(1)	0.5035(1)	0.1643(1)	0.5033(1)	0.014(1)
M9 = Sn9/Zn9	8*d*	0.52/0.48(1)	0.0698(1)	0.0902(1)	0.5081(1)	0.019(1)
M10 = Sn10/Zn10	4*c*	0.87/0.13(1)	0.2161(1)	$\frac{1}{4}$	0.6577(1)	0.033(1)
M11 = Sn11/Zn11	4*c*	0.62/0.38(1)	0.1060(1)	$\frac{1}{4}$	0.7492(1)	0.032(1)
M12 = Sn12/Zn12	8*d*	0.66/0.34(1)	0.9728(1)	0.1489(1)	0.7788(1)	0.028(1)
M13 = Sn13/Zn13	8*d*	0.71/0.29(1)	0.7842(1)	0.1553(1)	0.5816(1)	0.020(1)
Sn14	8*d*		0.8758(1)	0.0552(1)	0.6841(1)	0.020(1)
Sn15	4*c*		0.0987(1)	$\frac{1}{4}$	0.2548(1)	0.014(1)
Sn16	4*c*		0.1242(1)	$\frac{1}{4}$	0.4583(1)	0.017(1)
Sn17	8*d*		0.3364(1)	0.0946(1)	0.2069(1)	0.016(1)
Sn18	4*c*		0.3323(1)	$\frac{1}{4}$	0.1308(1)	0.016(1)
Zn14	4*c*		0.1997(1)	$\frac{1}{4}$	0.3514(1)	0.020(1)
Zn15	4*c*		0.9274(1)	$\frac{1}{4}$	0.2589(1)	0.020(1)
Zn16	8*d*		0.5100(1)	0.9257(1)	0.3907(1)	0.014(1)
Zn17	8*d*		0.1841(1)	0.1603(1)	0.1644(1)	0.020(1)
Zn18	8*d*		0.1939(1)	0.1022(1)	0.2806(1)	0.019(1)
Na1	8*d*		0.2223(2)	0.0648(2)	0.4190(1)	0.023(1)
Na2	4*c*		0.3293(2)	$\frac{1}{4}$	0.4575(2)	0.021(1)
Na3	4*c*		0.0127(2)	$\frac{1}{4}$	0.1277(2)	0.023(1)
Na4	8*d*		0.0149(2)	0.0636(2)	0.2181(1)	0.027(1)
Na5	8*d*		0.3021(2)	0.0622(2)	0.0545(1)	0.031(1)
Na6	4*c*		0.6072(3)	$\frac{1}{4}$	0.6143(2)	0.028(1)
Na8	4*c*		0.9275(3)	$\frac{1}{4}$	0.4944(2)	0.037(1)
Na9	4*c*		0.1847(3)	$\frac{1}{4}$	0.0320(2)	0.025(1)
Na10	4*c*		0.8054(3)	$\frac{1}{4}$	0.7185(2)	0.034(1)
Na11	8*d*		0.0187(2)	0.1266(2)	0.3674(1)	0.033(1)
Na12	8*d*		0.3320(2)	0.9366(2)	0.3107(1)	0.032(1)
Na13	8*d*		0.1961(2)	0.9435(2)	0.1744(1)	0.031(1)
Na14	4*c*		0.6111(3)	$\frac{3}{4}$	0.3917(2)	0.029(1)
Na15	8*d*		0.0796(2)	0.0820(2)	0.6564(1)	0.038(1)
Na16	4*c*		0.9758(6)	$\frac{1}{4}$	0.6291(4)	0.104(3)

Table 2 (*continued*)

Atom	Wyck.	Occ.≠1	*x*	*y*	*z*	U_{eq} (Å^2)
III						
Sn1	18*h*		0.5698(1)	0.4302(1)	0.1337(1)	0.014(1)
M2 = Sn2/Zn2	6*c*	0.45/0.55(2)	$\frac{2}{3}$	$\frac{1}{3}$	0.2198(1)	0.015(1)
M3 = Sn3/Zn3	18*h*	0.78/0.22(2)	0.4441(1)	0.5559(1)	0.0517(1)	0.013(1)
Sn4	3*a*		$\frac{2}{3}$	$\frac{1}{3}$	$\frac{1}{3}$	0.018(1)
M5 = Sn5/Zn5	18*h*	0.51/0.49(2)	0.4210(1)	0.5790(1)	0.1809(1)	0.014(1)
M6 = Sn6/Zn6	18*h*	0.19/0.81(2)	0.3866(1)	0.6134(1)	0.1087(1)	0.015(1)
M7 = Sn7/Zn7	18*h*	0.47/0.53(2)	0.5096(1)	0.4904(1)	0.1953(1)	0.015(1)
M8 = Sn8/Zn8	36*i*	0.66/0.34(2)	0.4479(1)	0.3689(1)	0.2552(1)	0.018(1)
M9 = Sn9/Zn9	18*h*	0.24/0.76(2)	0.4868(1)	0.2434(1)	0.2330(1)	0.017(1)
M10 = Zn10/Sn10	36*i*	0.68/0.32(1)	0.6327(1)	0.6412(1)	0.0364(1)	0.019(1)
M11 = Zn11/Sn11	36*i*	0.58/0.42(2)	0.3295(1)	0.4918(1)	0.9863(1)	0.020(1)
Zn12	18*h*		0.7214(1)	0.4427(2)	0.1628(1)	0.016(1)
Zn13	18*h*	0.87(1)	0.6094(1)	0.3906(1)	0.2768(1)	0.021(1)
Zn14	18*h*		0.5397(1)	0.4603(1)	0.0645(1)	0.020(1)
Zn15	36*i*		0.4132(1)	0.2969(1)	0.1794(1)	0.017(1)
Na1	36*i*		0.5843(4)	0.6227(4)	0.1226(2)	0.021(1)
Na2	18*h*		0.2220(3)	0.4441(6)	0.0642(2)	0.021(2)
Na3	6*c*		$\frac{1}{3}$	$\frac{2}{3}$	0.0294(4)	0.024(3)
Na4	18*h*		0.4112(8)	0.2056(4)	0.3226(3)	0.045(3)
Na5	18*h*		0.7964(4)	0.5928(7)	0.0968(3)	0.046(3)
Na6	6*c*		$\frac{2}{3}$	$\frac{1}{3}$	0.0749(5)	0.047(5)

Table 3
Ranges of interatomic distances (⩽4 Å) for different atom types in $Na_{16}Zn_{13.54}Sn_{13.46(5)}$ (**I**), $Na_{22}Zn_{20}Sn_{19(1)}$ (**II**), and $Na_{34}Zn_{66}Sn_{38(1)}$ (**III**).

Atom types		Distance range (Å)	Atom types		Distance range (Å)	Atom types		Distance range (Å)
I								
Sn	Sn	3.014(1)–3.077(1)	Zn	M	2.768(1)–2.906(1)	Na	Zn	3.183(3)–3.614(5)
Sn	Zn	2.726(1)–2.930(2)	M	M	2.602(2)–2.809(2)	Na	M	3.127(4)–3.487(4)
Sn	M	2.882(1)–2.978(1)	Na	Sn	3.149(3)–3.508(4)	Na	Na	3.421(1)–3.975(5)
Zn	Zn	2.644(1)–2.845(1)						
II								
Sn	Sn	2.976(1)	Zn	M	2.660(1)–2.881(1)	Na	Zn	3.204(4)–3.557(3)
Sn	Zn	2.721(1)–2.947(1)	M	M	2.670(2)–3.157(1)	Na	M	3.048(4)–3.995(4)
Sn	M	2.899(1)–3.176(1)	Na	Sn	3.208(4)–3.671(5)	Na	Na	3.152(9)–3.954(4)
Zn	Zn	2.789(1)–2.809(1)						
III								
Sn	Sn	–	Zn	M	2.645(3)–2.986(2)	Na	Zn	3.165(6)–3.62(2)
Sn	Zn	2.677(3)–3.000(2)	M	M	2.652(1)–3.031(3)	Na	M	3.170(6)–3.70(1)
Sn	M	2.877(2)	Na	Sn	3.175(6)–3.691(8)	Na	Na	3.508(7)–3.99(1)
Zn	Zn	2.527(3)–3.970(2)						

refined in the trigonal space group $R\bar{3}m$ (No. 166). Solutions in other monoclinic or the centrosymmetric space group $R\bar{3}$ resulted in comparable structure models therefore the solution in the higher symmetric $R\bar{3}m$ was chosen. Structure solution and refinement shows two Sn, four Zn, nine M sites that are statistically occupied by Sn and Zn (M2, M3, M5–M11 with Sn occupancies ranging from 19% to 78%), and six independent Na atoms. Zn13 was refined with 87% occupancy. Tables with ADPs of all compounds are provided as supplementary data (Table S1). Further details of the crystal structure investigations can be obtained from the Fachinformationszentrum Karlsruhe, 76344 Eggenstein–Leopoldshafen, Germany, (fax: +49 7247 808 666; e-mail: crysdata@fiz.karlsruhe.de) on quoting the depository number CSD 419872, 419873, and 419877 for compounds **I**, **II**, and **III**, respectively.

2.3. Scanning electron microscopy

After lattice parameter determination of single crystals of **I**, **II**, and **III** a standardless quantitative chemical analysis was carried out using a JEOL 5900LV electron microscope (accelerating voltage 20 kV, 3 min measuring times on five spots per crystal) equipped with a Röntec detector system for EDX analysis. The presence of only Na, Sn, and Zn and no other element heavier than boron was detected. The mean compositions obtained are Na:Zn:Sn = 42(5):30(7):28(3), 35(5):33(2):32(1), and 26(4):52(6):22(3) for **I**, **II**, and **III**, respectively. Within standard deviations the values are close to the calculated numbers (Na:Zn:Sn = 37.2:31.5:31.3, 36.1:32.8:31.1, and 24.6:47.8:27.5 for **I**, **II**, and **III**, respectively).

3. Results and discussion

3.1. Crystal structures

The three sodium zinc stannides $Na_{16}Zn_{13.54}Sn_{13.46(5)}$ (**I**), $Na_{22}Zn_{20}Sn_{19(1)}$ (**II**), and $Na_{34}Zn_{66}Sn_{38(1)}$ (**III**) contain three-dimensional (3D) anionic cluster networks of linked $\{Zn_xSn_y\}$icosahedra and additional building blocks, which are described more detailed in the following.

Compound **I** crystallizes in a new orthorhombic structure type. As depicted in Fig. 1a the structure is a 3D network of two types of

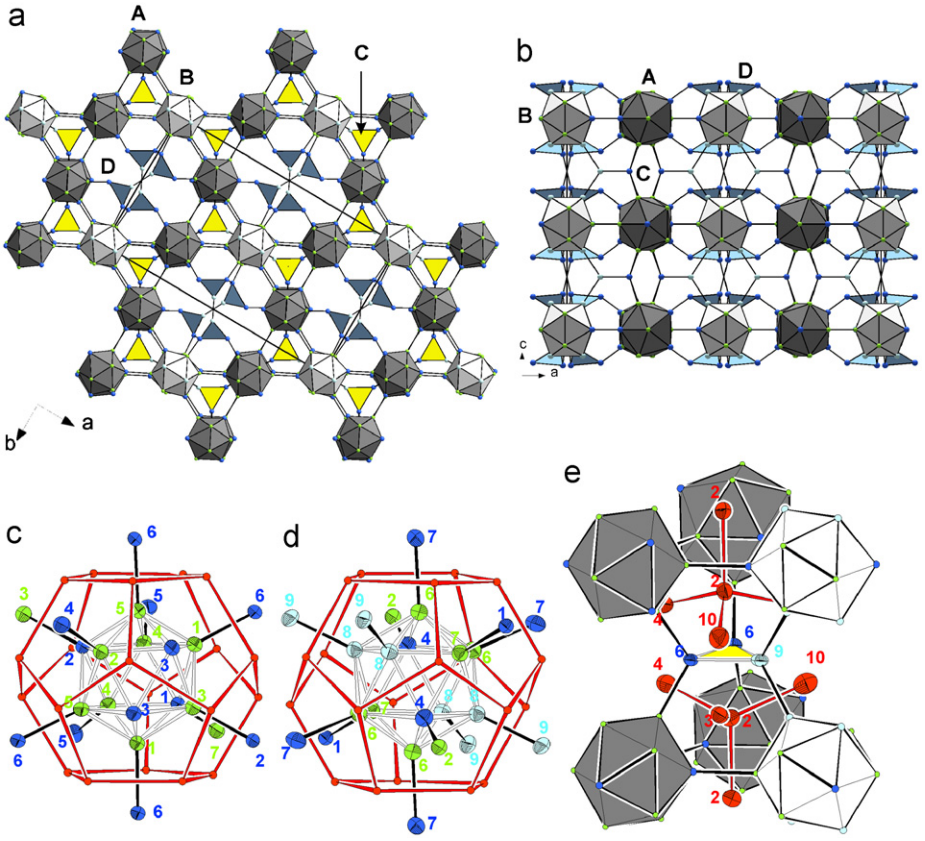

Fig. 1. Structural details for **I**: (a) projection of a Kagomé net of icosahedra **A** and **B** along **c** including of the unit cell axes. (b) View parallel to the Kagomé layers of icosahedra, which are stacked pseudo-primitive. (c) and (d) Icosahedra **A** and **B**, respectively, with surrounding {Na_{20}} pentagon dodecahedra (*pdod*). (e) Unit **C** interconnecting six icosahedra. All anisotropic representations of the atoms are drawn at 90% probability level. Na, Zn, Sn, and M = Zn/Sn atoms are represented with red, green, blue, and light blue color, respectively. Clusters **A**, **B**, **C**, and **D** are in gray, white, yellow, and blue, respectively. (For interpretation of the references to colour in this figure legend, the reader is referred to the web version of this article.)

icosahedra (**A** and **B**) and two triangles (**C** and **D**). Icosahedra **A** and **B** are directly connected and form (3.6.3.6) Kagomé nets in the *ab* plane. The layers lie at $z = 0$, and $\frac{1}{2}$ and are interlinked by triangular units **C** at $z = \frac{1}{4}$ and $\frac{3}{4}$ (Fig. 1b). The layer stacking *AA′AA′* along *c* is pseudo-primitive which leads to the formation of larger hexagonal and smaller triangular channels in this direction. Triangles **C** lie in the smaller, whereas in the bigger channels strands of interconnected triangles **D** are embedded (Fig. 1a). As shown in Fig. 1c all atomic positions Sn1–Sn3 and Zn1–Zn5 of **A** (with center on 8*j* site) are well ordered. The homoatomic intracluster distances Sn3–Sn3 and Zn–Zn are 3.014(1) and 2.644(1)–2.845(1) Å, respectively. The heteroatomic distances vary from 2.730(1) to 2.929(1) Å. Cluster **A** has 10 *exo*-bonds which connect adjoining clusters **A** (× 2), **B** (× 2), triangular units **C** (× 4), and **D** (× 2). All *exo*-bonds are heteroatomic and range from 2.726(1) to 2.832(1) Å. The Sn3 atoms have no *exo*-bonds.

Cluster **B** (with center on 4*c* site) consists of the atoms Sn4, Zn6, Zn7, and M8 (Fig. 1d). The intracluster bonds are Zn–Zn: 2.658(1) and 2.787(2) Å, Zn–Sn: 2.842(1) and 2.930(2) Å, M–Sn: 2.882(1) Å, M–Zn: 2.768(1)–2.906(1) Å, and the only M–M contact: 2.795(1) Å. All 12 atoms of cluster **B** have *exo*-bonds which connect the atoms to neighboring clusters **A** (× 4), **C** (× 4), and **D** (× 4) units. These bonds are formed via M8–M9 (2.780(1) Å) and Zn(Sn)–Sn(Zn) (2.729(1)–2.853(1) Å). Motif **C** is a triatomic ring of four-bonded (*4b*) atoms (Sn6–Sn6–M9). The triangle is slightly distorted with the smaller ring angle (59°) at Sn6 and the larger at M9 (~62°). The interatomic distances Sn6–Sn6 and M9–Sn6 are 3.069(1) and 2.978(1) Å, respectively. They are comparable to the Sn–Sn distance in cyclopropenyl like {Sn_3} in $BaSn_3$ (3.058 Å) [22]. As shown in Fig. 1e represents this entity the common face of two adjacent truncated tetrahedra which are aligned along *c*. Thus, ring **C** interlinks four units **A** and two units **B** through M9–M8 (2.780(1) Å) and Sn6–Zn1, Sn6–Zn5 bonds (2.774(1) and 2.832(1) Å, respectively). Finally, atoms Sn5, Sn7, and M10 compose the three-member unit **D** (Fig. 2c). Like in **C** we find the smaller valence angles 58.5–58.6° at Sn atoms and 62.8° at M10. Within this cluster the M–Sn bonds (2.889(1), 2.892(1) Å) are slightly shorter than the Sn5–Sn7 contact (3.013(1) Å). In contrast to **C**, which is exclusively composed of *4b* atoms, Sn5 is only three bonded and is connected to cluster **A** via Sn5–Zn4 (2.726(1) Å). Atom Sn7 establishes bonds to one unit **B** via Sn7–Zn6 (2.852(1) Å), and to adjoining **D** via Sn7–Sn7 (3.077(1) Å). M10–M10 bonds (2.602(2) and 2.809(2) Å) complete the coordination sphere of M10 atoms. Two units **D** together with each one triangular face of clusters **A** and **B** form the four triangular faces of a truncated tetrahedron (red polyhedra in Fig. 2a) which is centered by Na1. Along *c* pairs of these truncated tetrahedra—or Friauf polyhedra including four Na atoms (Na3 × 2, Na8, Na9)—are directly connected via Sn7–Sn7 and the connection between four **D** units creates a planar rectangle {M10}$_4$ with 90° bond angles. While single interlinking triangular motifs, such as **C** and pairs of triangles have been reported [23,24], the oligomerization of such triangles as in the present structure is novel.

The Na atoms are well separated from the clusters with shortest distances Na1–M10 = 3.127(4) Å. They form a pentagon dodecahedra (*pdod*) around **A** and **B** whereas the Na atoms around the four units **D** in the larger channels of the Kagome nets form an icosihexahedron. A similar {Na_{30}} cage around {Sn_{14}} units is found in $Na_{29}Zn_{24}Sn_{32}$ [10]. However, in the present case additional Na atoms cap pentagonal faces from the inside.

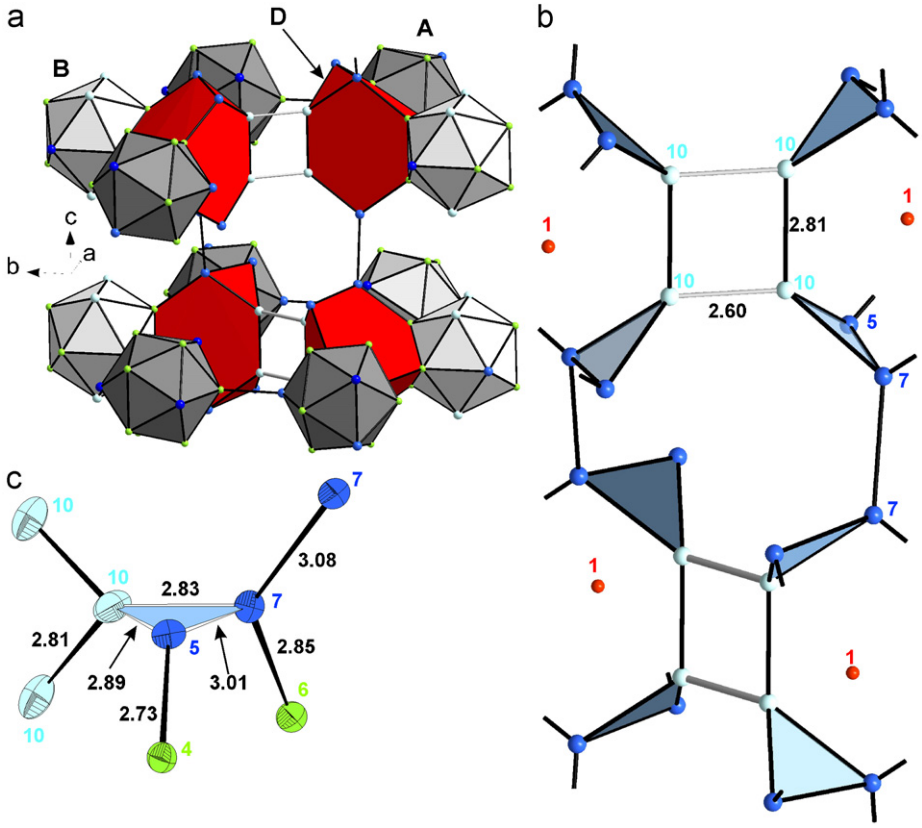

Fig. 2. Further structural details for **I**: (a) units **D** are part of truncated tetrahedra (shown in red) with adjacent icosahedra **A** and **B**. Two connected truncated tetrahedra fill the hexagonal channels of the Kagome net of icosahedra. (b) Atoms of the central unit of Fig. 2a emphasizing {M10} rectangles. (c) Anisotropic representation at 90% probability level of the atoms of **D** and connected atoms. Na, Zn, Sn, and M = Zn/Sn atoms are represented with red, green, blue, and light blue color, respectively. Clusters **A**, **B**, and **D** are in gray, white, and blue, respectively. (For interpretation of the references to colour in this figure legend, the reader is referred to the web version of this article.)

Compound **II** is structurally similar to Na_7Ga_{13}-II [16b] and $Na_{22}Ga_{39}$ [15] with equivalent atomic positions but larger unit cell parameters. The projection of the unit cell (Fig. 3a) shows the structure as an extended network of clusters, namely two types of icosahedra **E**, **F**, and a 15-atom spacer **G** in the ratio of 1:1:1. The structure can be easily understood in terms of a $MgCu_2$ *Laves* type structure by hierarchical cluster for atom replacement. As shown in Fig. 3b icosahedra **E** (gray) and icosahedra **F** (white) form (3.6.3.6) Kagome nets in the (101) plane. The layers are stacked in *ABCABC* sequence along [101] and are separated by 3^6 nets of type **E**. The role of Mg in $MgCu_2$ is taken by 15-atom spacers **G** (shown in blue), which are located in the large voids of the Kagome net and are connected in analogy to a cubic diamond sublattice (Fig. 3c,d). Unit **G** establishes several *exo*-bonds (see below) to the surrounding icosahedra and is embedded in a truncated super-tetrahedron composed of six clusters **E** and six clusters **F** (Fig. 4a). This feature is consistent with the 12(+4) coordination of Mg in $MgCu_2$.

Icosahedron **E** (center on site 4*c*) consists of the atoms Sn15, Sn18, Sn17, Zn14, Zn15, Zn17, Zn18, and M2 (Fig. 3e). The intracluster bonds M2–Zn18 and Sn17–Sn18 range from 2.770(1) to 2.976(1) Å. Nine *exo*-bonds are established to icosahedra **F** ($\times 4$) via Zn17–M1 (2.660(1) Å) and M2–M3 (2.701(1) Å); to other icosahedra **E** ($\times 2$) via Sn15–Zn15 and Zn15–Sn15 (2.811(1) Å); to unit **G** ($\times 3$) via Zn18–Sn14 (2.823(1) Å) and Zn14–Sn16 (2.720(1) Å). The atoms Sn17 and Sn18 have no *exo*-bonds. Icosahedron **F** (center on 4*a* site) consists of the atoms Zn16, M1, M3, M4, M7, and M8. Its intracluster bonds range from shorter M–Zn contacts (2.724(1)–2.881(1) Å) to longer M–M bonds (2.760(1)–2.938(1) Å). As shown in Fig. 3f it forms 12 *exo*-bonds to units **G** ($\times 6$) via Zn16–M12 (2.805(1) Å), M4–M5 (2.719(1) Å), and M7–M13 (2.808(1) Å); to unit **E** ($\times 4$) via M3–M2 (2.701(1) Å) and M1–Zn17 (2.660(1) Å); and to unit **F** ($\times 2$) via M8–M8 (2.674(1) Å). The interesting 15-vertex unit **G** that fills the structure is centered by Na16 (on site 4*c*) and consists of Sn14, Sn16, M5, M6, and M9 to M13 atoms (Fig. 4b). The unit derives from the 12-vertex truncated tetrahedron M6 ($\times 2$), M9 ($\times 2$), M10, M11, M12 ($\times 2$), M13 ($\times 2$), and Sn14 ($\times 2$). One of the triangular faces (see dashed lines in Fig. 4b) is capped by three further atoms M5 ($\times 2$) and Sn16. As a result the M10–M9 and M9–M9 contacts are enlarged and a deltahedral cap with four triangular faces is formed (Fig. 4b, top). The intracluster bonds are distributed to M–M (2.670(1)–3.157(1) Å) and M–Sn contacts (2.878(1)–3.176(1) Å). Spacer **G** has 13 *exo*-bonds. Four of them are to adjacent clusters **G** ($\times 2$) via M9–M6 and M6–M9 (2.795(1) Å). Three icosahedra **E** are bonded via two Sn14–Zn18 and one Sn16–Zn14 bonds (2.823(1) and 2.720(1) Å, respectively). Finally, six icosahedra **F** complete the coordination via M13–M7, M12–Zn16, and M5–M4 bonds (2.808(1), 2.805(1), and 2.719(1) Å, respectively). Vertices M10 and M11 are not *exo*-bonded. This emphasizes the relationship to $Na_{34}Zn_{66}Sn_{38(1)}$ **III** (see below), which also crystallizes in a $MgCu_2$ variant. Another parallel is the arrangement of Na atoms, which form pentagonal dodecahedra around **E** and **F** (shortest distances $\geqslant$3.048(4) Å d(Na14–M10)). Around **G** a {Na_{28}} hexacaidecahedron (*hkad*) appears with some faces capped by additional Na atoms from the inside (Fig. 4b, right). Similar to **III** this regular array of Na atoms forms a clathrate-II-type [25] network (Fig. 7c).

Phase **III** is isostructural to $Na_{102}Cu_{36}Ga_{279}$ [12] and is a new representative of triicosahedral phases [13]. The unit cell (Fig. 5a) is built up by icosahedra **H**, **J**, and a triply fused icosahedron **K** in the ratio 3:1:2. As the compound contains bigger and smaller

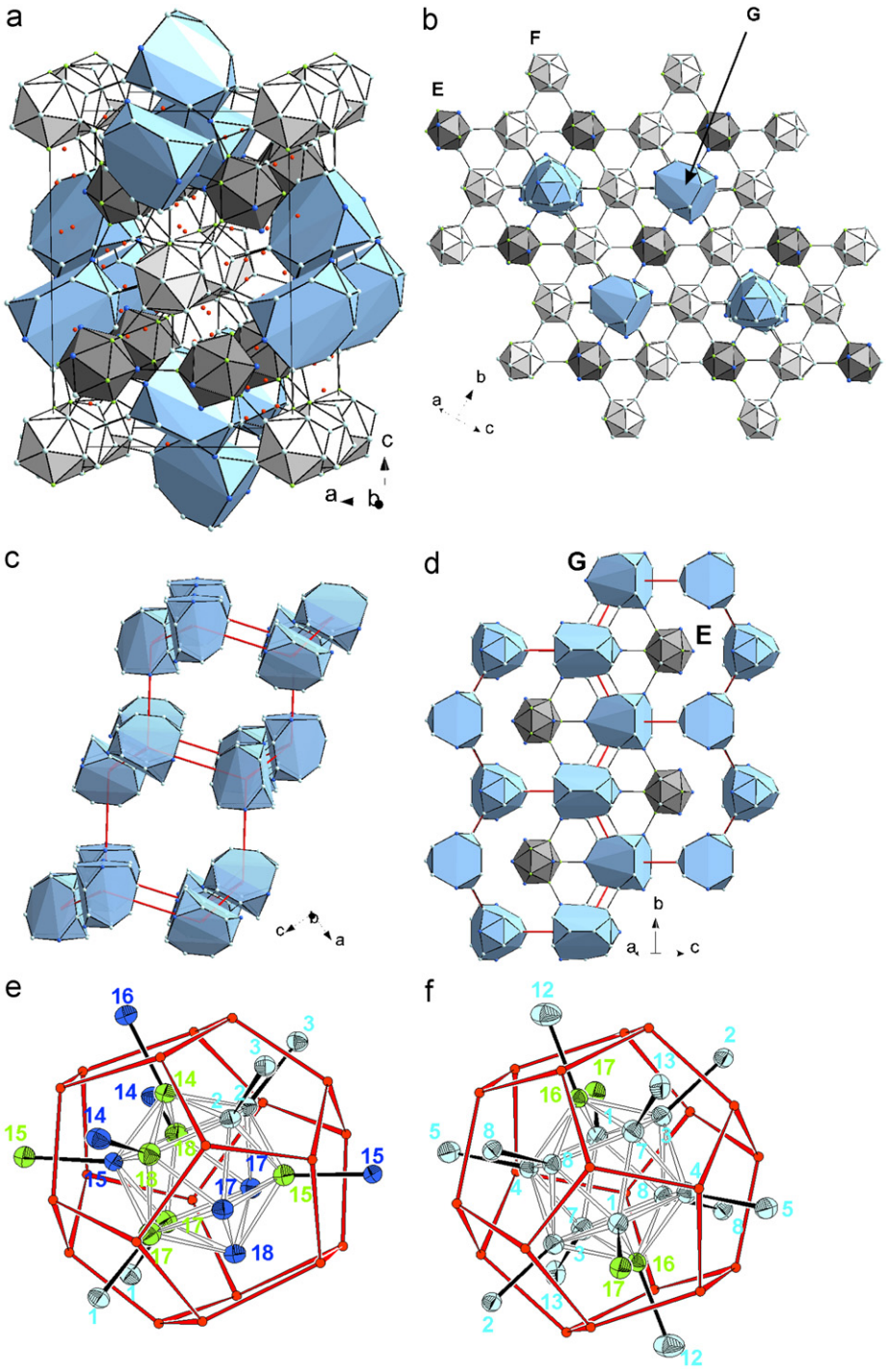

Fig. 3. Structural details for **II**: (a) polyhedral representation of the unit cell. (b) Kagome net made of **E** and **F** icosahedra. (c) and (d) Diamond substructure of **G** showing two orientations. (e) and (f) Icosahedra **E** and **F**, respectively, with surrounding $\{Na_{20}\}$ *pdods*. All anisotropic representations of the atoms are drawn at 90% probability level. Na, Zn, Sn, and M = Zn/Sn atoms are represented with red, green, blue, and light blue color, respectively. Clusters **E**, **F**, and **G** are in gray, white, and blue, respectively. (For interpretation of the references to colour in this figure legend, the reader is referred to the web version of this article.)

clusters in the ratio of 1:2 the 3D structure can again be understood as a hierarchical variant of cubic $MgCu_2$ in which each copper atom is replaced by a icosahedron and each Mg atom by cluster **K**. Unit **H** forms (3.6.3.6) Kagomé layers in the (001) plane (Fig. 5b) which are interconnected by icosahedron **J** along *c*. The larger voids of the 3D framework of icosahedra are capped with units **K**, which are linked again analogous to the cubic diamond sublattice (Fig. 5c and d).

Icosahedron **H** (center on site 9*e*) consists of Zn14, M3, M10, and M11 (Fig. 5e). The Zn–M intracluster bonds range from 2.699(2) to 2.851(2) Å and are slightly shorter than the M–M intracluster bonds, which lie in the range of 2.765(2)–3.026(2) Å. The cluster has 12 *exo*-bonds which connect adjoining icosahedra **H** (× 4), two icosahedra **J** (× 2), and six units **K** (× 6). Those bonds are established via M11–M11 (2.834(3) Å), M3–M6 (2.696(2) Å), M10–M8 (2.670(2) Å), and Zn14–Sn1 (2.700(3) Å). Icosahedron **J** (center on site (3*b*)) is composed of M5 and M6 atoms (Fig. 5f). The intracluster bonds range from 2.707(3)–2.845(3) Å. The 12 *exo*-bonds point towards icosahedra **H** (× 6) and six triicosahedra **K** (× 6). They are established via M5–M7 (2.657(2) Å) and M6–M3

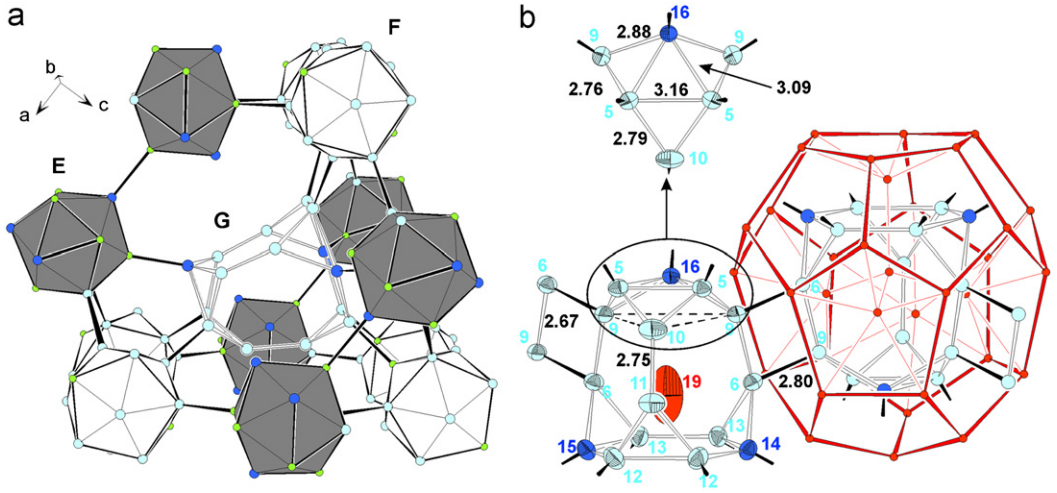

Fig. 4. Further structural details for **II**: (a) truncated supertetrahedron of twelve icosahedra around **G**. (b) Two interconnected units **G**. The 6-atom fragment of this unit is emphasized at the top of the picture. One $\{Na_{28}\}$ tetracaidecahedron (*tkad*) around **G** is shown with red lines. Ellipsoids are drawn at 90% probability level. Na, Zn, Sn, and M = Zn/Sn atoms are represented with red, green, blue, and light blue color, respectively. Clusters **E** and **F** are in gray and white, respectively. (For interpretation of the references to colour in this figure legend, the reader is referred to the web version of this article.)

(2.696(2) Å), respectively. The third eye catching 28-atom unit is a triply fused icosahedron **K** (Fig. 6c) composed of Sn1, Zn12, Zn13, Zn15, M2, and M7 to M9 atoms. This cluster is formed through the condensation of three icosahedral units (Fig. 6a), each of them sharing one triangular face (indicated with thick lines) with each of its neighbors and having one atom (M2, pink in Fig. 6b) in common. This building block has its structural analog in the β-boron structure. The intracluster separations involve 15 × Zn–Zn (2.682(3)–3.062(3) Å), 12 × Zn–Sn (2.694(1)–3.000(2) Å), 40 × Zn–M (2.645(3)–2.986(2) Å), 3 × Sn–M (2.877(2) Å), and 18 × M–M (2.685(2)–3.106(2) Å) contacts. Fig. 5d shows that six of the 18 *exo*-bonds are distributed to three other units **K** that are bonded in the *ab* plane via Zn15–Zn15 (2.527(3) Å). In the same plane three icosahedra **J** are coordinated via three M7–M5 bonds (2.657(2) Å). Nine icosahedra **H** that are bonded through M8–M10 (2.670(2) Å) and Sn1–Zn14 (2.700(3) Å) complete the coordination sphere. The defective (87% occ.) Zn13 apices (one of each participating icosahedron) form equilateral triangles (d(Zn13–Zn13) = 2.912(5) Å) which are interlinked by Sn4 (on site 3*a*). Thus, a sandwich complex $\{Sn(Sn_3Zn_{12}M_{13})_2\}$ with a six-fold-coordinate Sn4 in the center is realized (Fig. 6b). This extends the number of *exo*-bonds of **K** to (18+3). To our knowledge a Sn atom with a trigonal-antiprismatic coordination by Zn has not been observed yet. In similar phases containing such clusters, a transition metal atom—Cu or Cd—is located at the inversion center. Related triply fused icosahedra in gallides, such as in $Na_{13}K_4Ga_{49.57}$ [26], also frequently exhibit atomic defects preferably at the corresponding sites of the triangle made of the three defective Zn13 atoms and comparable complexes with a bridging atom have been found in the phases $Na_{102}Cu_{36}Ga_{279}$ [12], $K_{34}Li_{12.70}In_{92.30}$ [14], or the K–In–T (T = Mg, Au, Zn) phases [13]. Two other kinds of interaction between neighboring triply fused icosahedra dependent on the occupancy of the participating triangles have been reported: In $K_{34}In_{89.95(1)}Zn_{13.05(7)}$ [13] a bridging Zn–Zn dimer (occ. 42%) replaces the Sn4 position. In that case the 'Zn13' position is partially occupied (70%) and the triangle corresponds to a disordered dimer. In $Na_{13}K_4Ga_{49.57}$ [26] where the defect of the site corresponding to Zn13 is larger (occ. ~19%) no bridging atom or dimer is observed. In principle the stability of a non-defective triicosahedron inverted pair is increased with smaller and electron poorer elements, such as Zn, because the polyhedral geometry is relaxed by the resulting enlarged triangle [27]. The observed long Zn13–Zn13 separation (2.912(5) Å) is consistent with these arguments.

An alternative, more topological view of the structure is illustrated in Fig. 7. Icosahedron **J** fills a large 72 atom cage comprising 18 Zn (6 × Zn14, 12 × Zn15), 6 Sn1 and 48 M (6 × M3, 6 × M7, 12 × M8, 12 × M10, 12 × M11) atoms. The 72 atom cluster originates from a fullerane-like 60 atom cage with 12 atoms capping the five membered polygons of the fullerane from inside [27–29]. These pentagonal faces and the capping atoms are part of either icosahedra **H** or **K**. Filling of the fullerane originates from a central icosahedron **J** which is surrounded by 20 Na atoms that surmount the centers of the 20 triangular faces of **J** and form a *pdod*. 12 M (6 × M3 and 6 × M7) atoms cap the centers of the pentagonal faces of the *pdod* and are covalently bonded to the central icosahedron **J**. At the same time they cap the 12 pentagonal faces of the fullerane from the inside. The spheres of electropositive and electronegative elements resulting in the 104-atom Samson complex [30] can be formulated as $M_{12}@Na_{20}@M_{12}@$fullerane using an endohedral formalism. Following the packing of icosahedra **J** the present fullerane cages, with clusters **H** and **K** interlinking them, form close packed 3^6 layers in the *ab* plane and are stacked in the sequence *ABCABC* (Fig. 7b).

The Na atoms around unit **K** generate a $\{Na_{28}\}$ *hkad*. The latter is found in the ratio 1:2 with $\{Na_{20}\}$ *pdods* (which surround **H** and **J**), resulting in a $\{Na_{136}\}$ clathrate-II-type Na network (Fig. 7c) [25]. This regular arrangement of alkaline atoms around different sized clusters is frequently observed and is important for structure stabilization by filling space more efficiently and keeping the clusters apart [31].

3.2. Electron and bonding requirements

On the basis of the refined empirical formula and with respect to the site occupancy factors (Table 2) the formal average electron count for $\mathbf{Na_{16}Zn_{13.54}Sn_{13.46(5)}}$ can be performed as follows. All *exo*-bonds lie well in the range of 2*c*–2*e* bonds, thus, based on the 26 cluster electrons, which are required for a *closo*-cluster, the 10-fold *exo*-bonded icosahedron **A** has to be formulated as $\{Zn_8Sn_4\}^{8-}$, and the 12-fold *exo*-bonded icosahedron **B** as $\{Zn_{8.09}Sn_{3.91}\}^{6.18-}$. Assigning a formal charge of 0 and −2 to a (4*b*)Sn and a (4*b*)Zn, respectively, results in triangular unit **D**,

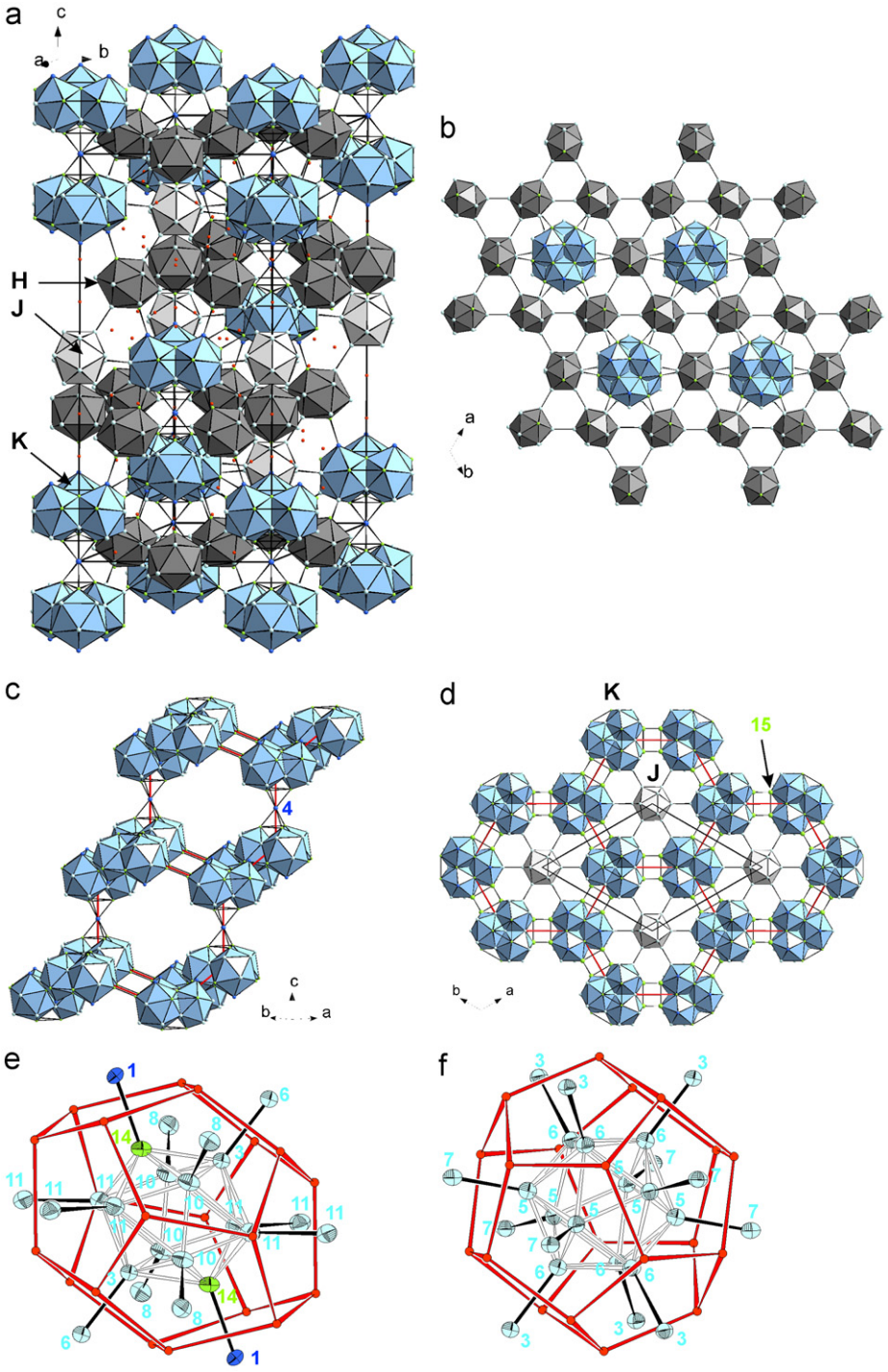

Fig. 5. Structural details for **III**: (a) polyhedral representation of the unit cell. (b) Kagome net made of **H**. (c) and (d) Diamond substructure of **K**. (e) and (f) Icosahedra **H** and **J** with surrounding $\{Na_{20}\}$ *pdods*. All anisotropic representations of the atoms are drawn at 90% probability level. Na, Zn, Sn, and M = Zn/Sn atoms are represented with red, green, blue, and light blue color, respectively. Clusters **H**, **J**, and **K** are in gray, white, and blue, respectively. (For interpretation of the references to colour in this figure legend, the reader is referred to the web version of this article.)

$\{Zn_{0.51}Sn_{2.49}\}^{2.02-}$ and triangular unit **C** $\{Zn_{0.48}Sn_{2.52}\}^{0.96-}$. Two formula units contain $2\times\mathbf{A}^{8-}$, $1\times\mathbf{B}^{6.18-}$, $2\times\mathbf{C}^{0.96-}$, and $4\times\mathbf{D}^{2.02-}$ which results in a total charge of ~32.18 electrons. Thus, number of Na atoms (32) is very close to the calculated value according to Zintl rules and the compound can be regarded as closed shell within the limits of the crystallographically determined composition. Longer annealing periods did not result in an ordering of the atomic positions so the observed disorder owes to the driving force for charge balance.

Due to the throughout statistical occupancy of Zn and Sn and the unusual bonding in the open polyhedron **G** the average electron count for $\mathbf{Na_{22}Zn_{20}Sn_{19(1)}}$ is difficult to assign. A Ga analog of this polyhedron has been found in Na_7Ga_{13}-I ($R\bar{3}m$) and Na_7Ga_{13}-II (*Pnma*) by Schäfer [16] and in $Na_{22}Ga_{39}$ (*Pnma*) by Belin [15]. In Na_7Ga_{13}-I cluster **G** is all *exo*-bonded, empty, and the bond corresponding to M10–M11 is in the range of normal covalent bond (2.55 Å). Therefore, Schäfer assigned 44 skeletal electrons to this polyhedron which leads to closed shell configuration as

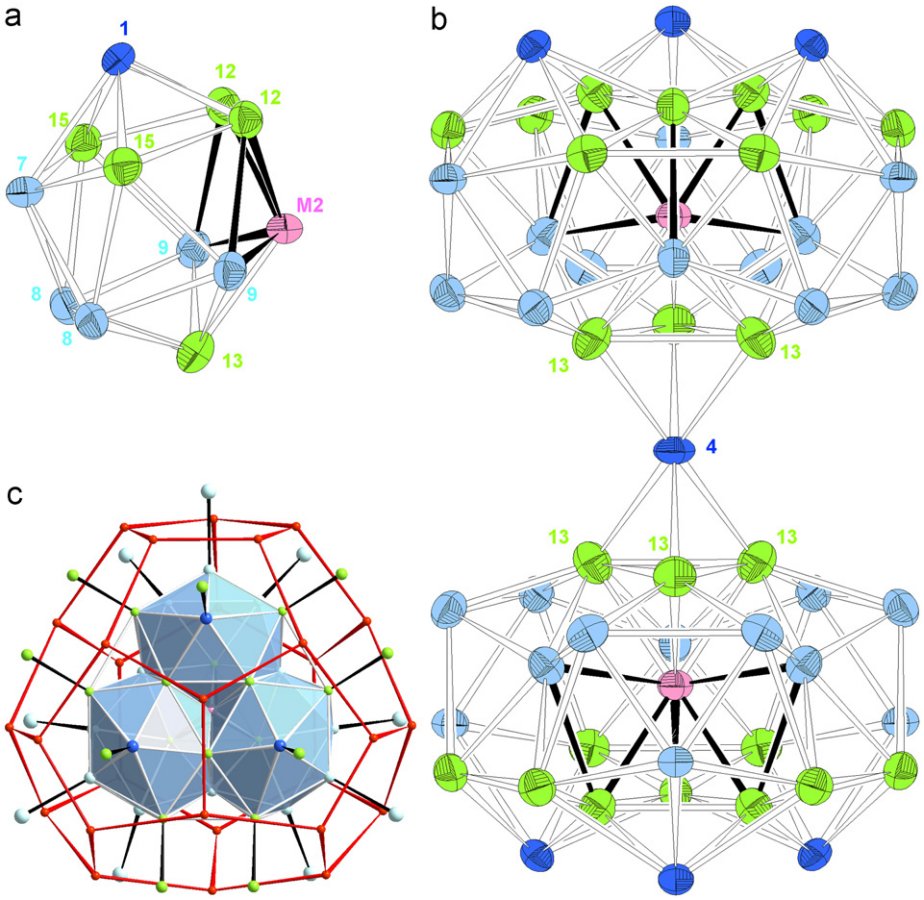

Fig. 6. Further structural details for **III**: (a) one of the three icosahedra that build up cluster **K** with the triply shared atom M2 (purple). (b) Pair of triply fused icosahedra **K**. The common icosahedra edges are outlined and the *exo*-bonds are omitted. (c) $\{Na_{28}\}$ *hkad* around **K**. All anisotropic representations of the atoms are drawn at 90% probability level. Na, Zn, Sn, and M = Zn/Sn atoms are represented with red, green, blue, and light blue color, respectively. (For interpretation of the references to colour in this figure legend, the reader is referred to the web version of this article.)

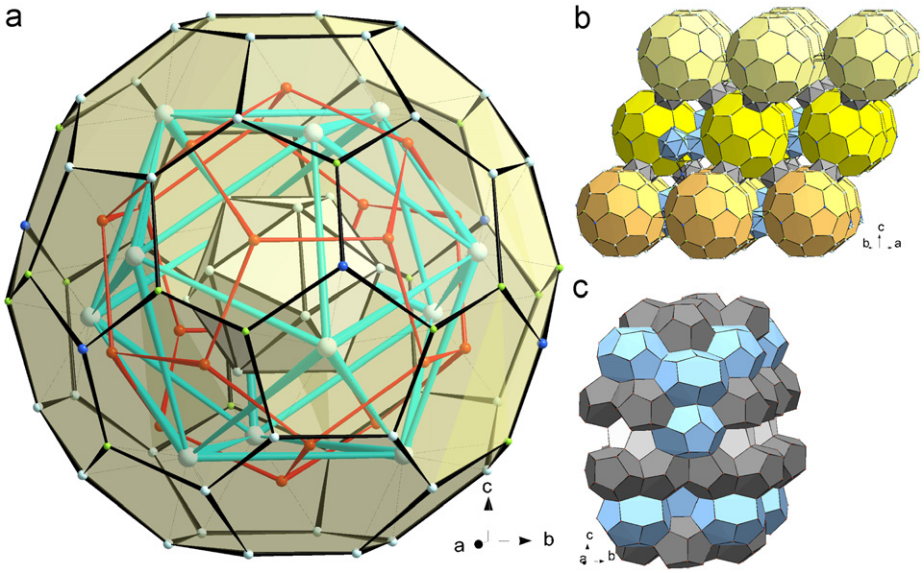

Fig. 7. Further structural details for **III**: (a) the 104 atom complex with central icosahedron **J**. (b) Packing of the fullerane cages. (c) The clathrate-II-type $\{Na_{136}\}$ network made of two kinds of $\{Na_{20}\}$ *pdods* (gray, around cluster **H** and white, around cluster **J**) and $\{Na_{28}\}$ *hkads* (blue, around cluster **K**). (For interpretation of the references to colour in this figure legend, the reader is referred to the web version of this article.)

confirmed by molecular orbital studies by Burdett [32]. In $Na_{22}Ga_{39}$ and Na_7Ga_{13}-II the cage has only 13 *exo*-bonds, is filled with a Na atom, and the Ga–Ga bond of interest is rather short (2.44 and 2.42 Å, respectively). In the case of $Na_{22}Ga_{39}$ Belin assigned 43 [33] and King 47 electrons [34]. According to Burdett [32] and under the assumption of a Ga = Ga double bond the

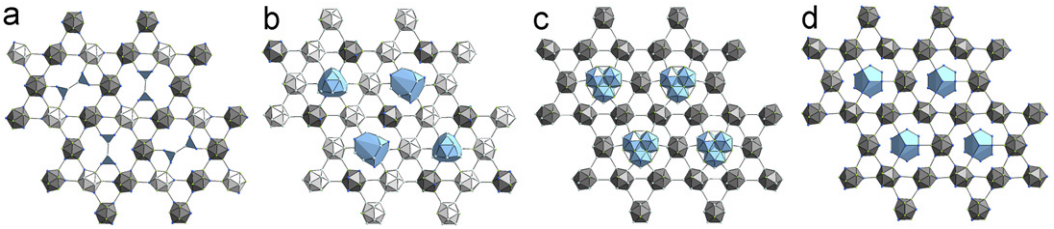

Fig. 8. Kagomé layers of icosahedra (gray and white clusters) and additional structure motifs (blue) in the compounds: (a) **I**, (b) **II**, (c) **III**, and (d) $Na_{29}Zn_{24}Sn_{32}$ [10]. (For interpretation of the references to colour in this figure legend, the reader is referred to the web version of this article.)

cluster requires 46 electrons. Whereas Burdett's results are in agreement for Na_7Ga_{13}-II, $Na_{22}Ga_{39}$ contains too much Na and has to be considered open shell (there are 556 electrons per unit cell but the number required is only 552, $Z=4$).

In $\mathbf{Na_{22}Zn_{20}Sn_{19(1)}}$ we observe features of both structures Na_7Ga_{13}-I and Na_7Ga_{13}-II/$Na_{22}Ga_{39}$. Cluster **G** is centered by Na16, has 13 *exo*-bonds, but the M10–M11 contact lies well in the range of a normal 2*c*–2*e* bond. We do not see any inconsistency in the refined Na content. Thus, based on the stoichiometry and with respect to the statistical occupancies icosahedron **E** is formulated as $\{Zn_{7.06}Sn_{4.94}\}^{7.12-}$ and cluster **F** results in $\{Zn_{8.27}Sn_{3.73}\}^{6.54-}$. Cluster **G** $\{Sn_{10.13}Zn_{4.87}\}$ has a total of 50.26 VE. Due to the typical single-bond length (d(M10–M11) = 2.749(1) Å) no double bond should be considered and the model with 44 skeletal electrons applies here. Taking into account the 13 *exo*-bonds and two electron lone pairs (at M10 and M11) a charge of −10.74 results for this unit. As clusters **E**, **F**, and **G** are present in the ratio 1:1:1 a total negative charge (electron demand) of 24.40 for the anionic network results. Those charges are counterbalanced by 22 Na atoms. Therefore, **III** corresponds to a closed shell phase with an electron deficiency of 2.40 electrons (or 1.10 electrons considering the error of the crystallographic composition within the 3σ range).

The average electron count of $\mathbf{Na_{34}Zn_{66}Sn_{38(1)}}$ can be derived by applying Wade's rules to the icosahedra and the *mno* rule [5e,f] to the sandwich complex. With respect to the mixed occupied vertices and the *exo*-bond requirements (both 12-fold) icosahedron **H** and **J** are formulated as $\{Zn_{7.48}Sn_{4.52}\}^{4.96-}$ and $\{Zn_{7.80}Sn_{4.20}\}^{5.60-}$, respectively. The complex unit (**K**–Sn4–**K**) requires $m+n+o = 57+8+1 = 66$ skeletal electron pairs or 132 electrons for stabilization [13,35]. Counting four electrons for Sn4 and subtracting 18×2 *exo*-bonds leads to the formulation $\{Sn(\square_{0.39}Sn_{9.54}Zn_{18.07})_2\}^{15.4-}$ ($\square$ = vacancy). Hence, per formula unit the number of valence electrons to fill all the bonding levels adds up to $3\times4.96+1\times5.60+1\times15.4 = 38.88$, which means an electron deficiency of 1.88. In other words, the total amount of valence electrons in the unit cell ($Z=3$) is 954 which is close to the demand of $12\times(26+12)+3\times(132+36) = 960$ electrons for a hypothetical network with four *12b*-icosahedra and one *36b*-$\{M(M_{28})_2\}$ unit.

So far only triicosahedral phases with an electron excess and E_F located above a gap in the DOS, meaning some electrons remain in the valence band of the alkali metals, have been reported, such as for $K_{34}In_{92.3}Li_{12.7}$, $K_{14}Na_{20}In_{91.82}Li_{13.18}$, or $K_{14}Na_{20}In_{96.3}$ [14] (all have ~970 electrons per unit cell). In those phases electronic tuning is realized by partial substitution of In by Li or by underoccupied vertices. Based on Extended Hückel calculations in those phases it has been found that the non-existence of any corresponding ordered $K_{34}In_{105}$ indicates only electron poorer lattices, as confirmed in the present case, than the ideal $A_{34}In_{105}$ to be stable, since 1034 ($Z=3$) electrons per unit cell would place E_F within strongly antibonding states. A comparable situation has been reported for $Na_{102}Cu_{36}Ga_{279}$ [12] and $K_4Na_{13}Ga_{49.57}$ [26], where the total available valence electrons also exceed the count required for lattice stabilization. Considering the standard deviations of the statistically occupied sites for $\mathbf{Na_{34}Zn_{66}Sn_{38(1)}}$, the compound might as well be charge balanced within 3σ-error values. Nevertheless, due to the multiple possible permutations the modeling of the statistical occupancies is rather difficult [36].

Based on the Na content compounds **I**–**III** have the formulae $NaZn_{0.85}Sn_{0.84}$ (**I**), $NaZn_{0.91}Sn_{0.86}$ (**II**), and $NaZn_{1.94}Sn_{1.12}$ (**III**). Including $Na_{29}Zn_{24}Sn_{32}$ (**IV**) (= $NaZn_{0.83}Sn_{1.10}$) [10] for comparison we find a nice trend of those structures based on the Kagomeé nets of icosahedra. Whereas **I** and **IV** form a primitive packing, **II** and **III** form icosahedra networks in the hierarchical Laves phase type (Fig. 8). The structures of the compounds in this region of the ternary phase system Na/Zn/Sn are very sensitive to composition and therefore to the valence electron concentration (VEC) using the Zintl formalism. A successive decrease in VEC per network atom (E) is observed in the order **IV**, **I**, **II**, and **III**. Whereas in **IV** (VEC = 3.66) the higher VEC leads to a structure with a covalently bonded substructure of exclusively Sn atoms (filling the hexagonal channels of the Kagomé net of icosahedra), the number of covalent and thus shorter E–E bonds is lower in **I** (VEC = 3.59) and **II** (VEC = 3.54), and completely disappears in **III** (VEC = 3.06), where clusters of triply fused icosahedra fill the network of icosahedra.

4. Conclusions

The presented three new intermetallic phases **I**–**III** show that in contrast to the binary Zn–Sn system compound formation between Zn and Sn atoms takes place in the anionic part of ternary compounds including also Na. **I**–**III** resemble structure motifs frequently found in binaries of Na and group-13 elements. Therefore, in those compounds the element Zn can be regarded as a pseudo *p*-block element and Zn/Sn mixing as isovalent with triel elements. Like their pendants in trielide chemistry the structures of the title phases show a distinct dependency on VEC and with respect to their compositions **I** and **III** are roughly balanced valence compounds according to the extended 8-N rule. The slight electron deficiency found for **II** and the existence of the electron richer $Na_{22}Ga_{39}$ [15] suggests a remarkable flexibility of the structure towards VEC.

Acknowledgment

We thank Dr. B. Wahl for discussions on the single crystal structure refinements.

Appendix A. Supplementary material

Supplementary data associated with this article can be found in the online version at doi:10.1016/j.jssc.2008.12.023.

References

[1] [a] H. Schäfer, J. Solid State Chem. 57 (1985) 97;
[b] H.G. von Schnering, Angew. Chem. 93 (1981) 44;
[c] S.M. Kauzlarich (Ed.), Chemistry, Structure and Bonding of Zintl Phases and Ions, VCH, 1996.
[2] F. Laves, Theory of Alloys Phases, ASM, Cleveland, OH, 1956.
[3] M. Tillard-Charbonnel, C. Belin, Prog. Solid State Chem. 22 (1993) 59 and references therein.
[4] H.C. Longuet-Higgins, M. de V. Roberts, Proc. R. Soc. A 230 (1955) 110.
[5] [a] W.N. Lipscomb, Boron Hydrides, Benjamin, New York, 1963;
[b] B.K. Teo, Inorg. Chem. 23 (1984) 1251;
[c] B.K. Teo, Polyhedron 9 (1990) 1985;
[d] D.M.P. Mingos, Acc. Chem. Res. 17 (1984) 311;
[e] M.M. Balakrishnarajan, E.D. Jemmis, J. Am. Chem. Soc. 122 (2000) 4516;
[f] E.D. Jemmis, M.M. Balakrishnarajan, P.D. Pancharatna, Chem. Rev. 102 (2002) 93.
[6] J.K. Burdett, E. Canadell, Inorg. Chem. 30 (1991) 1991.
[7] Q. Lin, J.D. Corbett, Inorg. Chem. 44 (2005) 512.
[8] [a] M. Charbonnel, C. Belin, J. Solid State Chem. 64 (1987) 210;
[b] M. Charbonnel, C. Belin, J. Solid State Chem. 67 (1987) 210.
[9] [a] K. Wade, Adv. Inorg. Radiochem. 21 (1976) 711;
[b] D.M.P. Mingos, Nat. Phys. Sci. 236 (1972) 99;
[c] R.E. Williams, Inorg. Chem. 10 (1971) 210;
[d] R.W. Rudolph, Acc. Chem. Res. 9 (1976) 446.
[10] S.-J. Kim, S.D. Hoffmann, T.F. Fässler, Angew. Chem. Int. Ed. 46 (2007) 3144.
[11] [a] E. Todorov, S.C. Sevov, J. Am. Chem. Soc. 119 (1997) 2869;
[b] E. Todorov, S.C. Sevov, Inorg. Chem. 36 (1997) 4298.
[12] M. Tillard-Charbonnel, N. Chouaibi, C. Belin, J. Lapasset, J. Solid State Chem. 100 (1992) 220.
[13] B. Li, J.D. Corbett, Inorg. Chem. 45 (2006) 8958.
[14] B. Li, J.D. Corbett, J. Am. Chem. Soc. 127 (2005) 926.
[15] R.G. Ling, C. Belin, Acta Crystallogr. 38B (1982) 1101.
[16] [a] U. Frank-Cordier, G. Cordier, H. Schäfer, Z. Naturforsch. 37B (1982) 119;
[b] U. Frank-Cordier, G. Cordier, H. Schäfer, Z. Naturforsch. 37B (1982) 127.
[17] G. Cordier, V. Müller, Z. Kristallogr. 198 (1992) 302.
[18] S.-J. Kim, F. Kraus, T.F. Fässler, J. Am. Chem. Soc., in press.
[19] ABSPACK, Oxford Diffraction Ltd., Abingdon, UK, 2005.
[20] [a] G.M. Sheldrick, SHELXS-97, Program for the Solution of Crystal Structures, Universität Göttingen, Germany, 1997;
[b] G. Sheldrick, SHELXL-97, Program for the Refinement of Crystal Structures, Universität Göttingen, Germany, 1997.
[21] From a different reaction a structure with a partially occupied Na position at the center of four units D and less tin content was found. Structure solution of that compound resulted in: $a = 27.487(6)$, $b = 16.075(3)$, $c = 18.484(4)$ Å, R_1/wR_2 (all data) = 0.042/0.090.
[22] C. Kronseder, T.F. Fässler, Angew. Chem. Int. Ed. 36 (1997) 2683.
[23] D.M. Flot, M. Tillard-Charbonnel, C. Belin, J. Am. Chem. Soc. 118 (1996) 5229.
[24] S.C. Sevov, J.D. Corbett, J. Solid State Chem. 103 (1993) 114.
[25] [a] W.F. Claussen, J. Chem. Phys. 19 (1951) 1425;
[b] T.F. Fässler, Angew. Chem. 46 (2000) 2572;
[c] S. Bobev, S.C. Sevov, J. Solid State Chem. 153 (2000) 92.
[26] C. Belin, M. Charbonnel, J. Solid State Chem. 64 (1986) 57.
[27] C. Belin, M. Tillard-Charbonnel, Coord. Chem. Rev. 178–180 (1998) 529.
[28] S.C. Sevov, J.D. Corbett, Science 262 (1993) 880.
[29] R. Nesper, Angew. Chem. Int. Ed. 33 (1994) 843.
[30] [a] S. Samson, in: A. Rich, N. Davidson (Eds.), Structural Chemistry and Molecular Biology, Freeman, San Francisco, 1968, p. 687;
[b] L. Pauling, Proc. Natl. Acad. Sci. USA 84 (1987) 3537;
[c] R.B. King, Inorg. Chim. Acta 181 (1991) 217.
[31] J.D. Corbett, Angew. Chem. Int. Ed. 39 (2000) 670.
[32] J. Burdett, E. Canadell, J. Am. Chem. Soc. 112 (1990) 7207.
[33] C. Belin, R.G. Ling, J. Solid State Chem. 48 (1983) 40.
[34] R.B. King, Inorg. Chem. 28 (1989) 2796.
[35] M. Tillard-Charbonnel, A. Manteghetti, C. Belin, Inorg. Chem. 39 (2000) 1684.
[36] [a] K. Nordell, G.J. Miller, Inorg. Chem. 38 (1999) 579;
[b] G.J. Miller, Eur. J. Inorg. Chem. (1998) 523;
[c] B.K. Teo, H. Zhang, Y. Kean, H. Dang, X. Shi, J. Chem. Phys. 99 (1993) 2929.